Preprint
UCRL-JRNL-201009

Nondipole effects in the photoionization of Xe $4d_{5/2}$ and $4d_{3/2}$: Evidence for quadrupole satellites

O. Hemmers,[1] R. Guillemin,[1,2] D. Rolles,[2,3] A. Wolska,[1,2] D. W. Lindle,[1] K. T. Cheng,[4] W. R. Johnson,[5] H. L. Zhou,[6] and S. T. Manson[6]

[1]University of Nevada, Las Vegas, NV 89154
[2]Advanced Light Source, Lawrence Berkeley National Laboratory, Berkeley, CA 94720
[3]Fritz-Haber-Institut der Max-Planck-Gesellschaft, D14195 Berlin, Germany
[4]Lawrence Livermore National Laboratory Livermore, CA 94550
[5]University of Notre Dame, Notre Dame, IN 46556
[6]Georgia State University, Atlanta, CA 30303

U.S. Department of Energy

Lawrence Livermore National Laboratory

This article was submitted to the Physical Review Letters

November 2003

DISCLAIMER

Nondipole effects in the photoionization of Xe $4d_{5/2}$ and $4d_{3/2}$: Evidence for quadrupole satellites

O. Hemmers,[1] R. Guillemin,[1,2] D. Rolles,[2,3] A. Wolska,[1,2] D. W. Lindle,[1]
K. T. Cheng,[4] W. R. Johnson,[5] H. L. Zhou,[6] and S. T. Manson[6]

[1] *Department of Chemistry, University of Nevada, Las Vegas, NV 89154-4003*
[2] *Advanced Light Source, Lawrence Berkeley National Laboratory, Berkeley, California 94720*
[3] *Fritz-Haber-Institut der Max-Planck-Gesellschaft, D-14195 Berlin, Germany*
[4] *University of California, Lawrence Livermore National Laboratory, Livermore, California 94550*
[5] *Department of Physics, University of Notre Dame, Notre Dame, Indiana 46556*
[6] *Department of Physics and Astronomy, Georgia State University, Atlanta, GA 30303-3083*

Strong evidence for the existence and importance of quadrupole satellite transitions is found in spin-orbit-resolved Xe $4d$ nondipole photoionization in a combined experimental/theoretical study.

PACS numbers: 31.25.Eb, 32.80.Fb

Over the past decade or so there has been an upsurge in both experimental and theoretical studies of nondipole effects in atomic and molecular photoionization [1–13] owing to advances in experimental capabilities, notably third-generation synchrotron light sources. These studies have revealed significant nondipole effects not only at multi-keV photon energies but at hundreds and even tens of eV [1, 5–13]. The nondipole effects in photoionization show up clearly in photoelectron angular distributions due to the dependence of the differential cross section on interferences among the continuum waves resulting from the absorption of photons of various multipolarities, most commonly between dipole and quadrupole channels. A great deal is known about dipole photoionizing transitions in atoms [14, 15], while far less is known about the corresponding *quadrupole* transitions. Thus, in addition to the intrinsic interest in photoelectron angular distributions, studies of nondipole angular-distribution effects provide information on the relatively weak ionizing quadrupole transitions, both their amplitudes and their phases, information which is otherwise inaccessible. Of particular interest here is quadrupole transitions in photoionization connect the initial discrete state of the photoionization process to final continuum states of different angular momentum and parity from those connected by dipole transitions, thereby facilitating study of the quadrupole-allowed continua.

In this Letter, we report on a combined experimental/theoretical study of the differential photoionization cross sections for Xe $4d_{5/2}$ and $4d_{3/2}$ channels, showing large nondipole contributions and dynamical differences between the spin-orbit-split channels, thereby highlighting the important dynamical contribution of relativistic effects. The results exhibit large discrepancies between theory and experiment. The most likely explanation for these discrepancies is the existence and importance of quadrupole satellite channels–this is the first time effects of multiple-electron transitions in the quadrupole manifold have been observed.

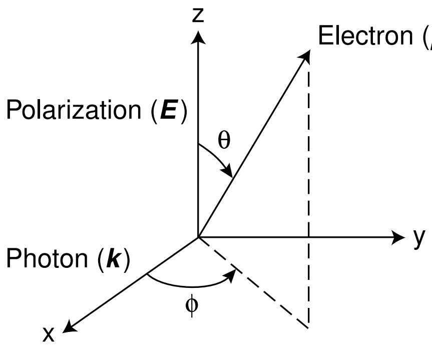

FIG. 1: Geometry applicable to photoelectron angular-distribution measurements using polarized light.

The differential photoionization cross section, including the lowest-order nondipole contributions which arise owing to the interference between dipole and quadrupole photoionization channels, is given by [2, 3, 16–19]

$$\frac{d\sigma}{d\Omega}(\theta,\phi) = \frac{\sigma}{4\pi}\left\{1+\beta P_2(\cos\theta)+(\delta+\gamma\cos^2\theta)\sin\theta\cos\phi\right\}, \tag{1}$$

where σ is the angle-integrated cross section, β is the dipole anisotropy parameter, $P_2(\cos\theta)=(3\cos^2\theta-1)/2$, and δ and γ are nondipole anisotropy parameters. As depicted in Fig. 1, the coordinate axes have the positive x-axis along the direction of the photon propagation vector, the z-axis along the photon polarization vector, and θ and ϕ are the polar and azimuthal angles of the photoelectron momentum vector. The nondipole parameters, δ and γ, are given by linear combinations of $(\mathrm{Q}_i/\mathrm{D}_j)\cos\delta_{ij}$ with Q_i and D_j the quadrupole and dipole matrix elements, respectively, and the δ_{ij} are phase shift differences [3, 19].

Measurements over the 100–250 eV photon energy range were made at the Advanced Light Source (ALS) of the Lawrence Berkeley National Laboratory during three different experimental campaigns. The experiments were performed on undulator beamline 8.0.1.3 using a gas-phase time-of-flight (TOF) electron-spectroscopy system [20]. The TOF method can measure photoelectron peaks at many kinetic energies and at multiple emission angles simultaneously, permitting sensitive determinations of electron angular distributions with minimal experimental uncertainty. Retarding voltages between -80 V (hν=100 eV) and -190 V (hν=250 eV) were applied to slow the electrons in order to resolve the two Xe $4d$ lines. Ne $2s$, Ar $2p$, and He $1s$ photolines were used to calibrate the analyzer transmissions because the dipole and nondipole contributions to their angular distributions are now well known. The degree of linear polarization of the synchrotron light was determined to be > 99.9 %. The electron analyzers were positioned at sets of angles sensitive to different combinations of the angular anisotropy parameters β, δ, and γ, and differences in the photoelectron intensities yielded values of the combined nondipole parameter $\zeta = \gamma + 3\delta$. The experimental geometry is most conducive to the measurement of ζ, so it is ζ we usually study.

Calculations were carried out using relativistic random-phase approximation (RRPA) methodology [21, 22]. RRPA includes significant aspects of ground-state correlation, along with interchannel coupling among all of the photoionization channels that are included. In the present work, *all* relativistic single ionization and excitation channels from the $4s$, $4p_{1/2}$, $4p_{3/2}$, $4d_{3/2}$, $4d_{5/2}$, $5s$, $5p_{1/2}$, and $5p_{3/2}$ subshells of Xe are considered, a total of 20 interacting dipole and 25 interacting quadrupole channels. This calculation is entirely *ab initio* except *experimental* binding energies have been used. This methodology has been found to give excellent results for Xe $4d$ dipole photoionization [23] and Xe $5s$ nondipole photoionization [13], both in the same energy range considered herein.

The experimental results for the nondipole ζ parameter are shown in Fig. 2 as a function of photoelectron energy. A notable feature of the measurement is the $4d_{3/2}$ nondipole parameter reaches a value of about -0.6, and the $4d_{5/2}$ nondipole parameter reaches a value of about -0.5, at a photoelectron energy of about 110 eV, which corresponds to a photon energy of about 180 eV, the region just above the $4p$ thresholds. In other words, in both cases, the nondipole contribution to the photoelectron differential cross section is of the same order of magnitude as the purely dipole contribution characterized by the parameter β in Eq. 1. To get a better idea of the importance of the nondipole effects, using Eq. 1 for a value of θ of 54.7 degrees (the "magic angle"), the backward (ϕ = 180 degrees) flux exceeds the forward (ϕ = 0 degrees) by about 40 %; without the nondipole contribution to the differential cross section, this difference vanishes, emphasizing the importance of nondipole effects even at such low energies. Furthermore, a measurable difference is seen between the ζ parameters for $4d_{3/2}$ and $4d_{5/2}$ channels, which are plotted vs. photoelectron energy to obviate any differences arising from the differing threshold energies of the two channels. This demonstrates dynamical differences between the $4d_{3/2}$ and $4d_{5/2}$ channels, i.e., differences in radial wave functions, indicating relativistic effects must be included for correct dynamics. So far as we know, this is the first experimental determination of such dynamical differences in nondipole photoionization arising from relativistic effects. Finally, the large values of the nondipole parameter persist for nearly 100 eV above the $4p$ thresholds.

Also shown in Fig. 2 are the results of our RRPA calculations. Below a photoelectron energy of about 80 eV, the theoretical result is in excellent agreement with experiment. At higher energies, from about 80 eV to 180 eV, starting around the $4p$ ionization thresholds, agreement is poor; the experiment shows a broad region in which the nondipole parameter ζ takes on large negative values, then slowly increases with increasing energy. The theoretical result, on the other hand, shows significant differences in the behaviors of the $4d_{3/2}$ and $4d_{5/2}$ channels only in the immediate neighborhood of the $4p$ thresholds, followed by a rapid rise to small *positive* values of ζ and a slightly decreasing plateau region. This disagreement is quite surprising in view of the excellent agreement found for the nondipole parameter in the case of Xe $5s$ photoionization in the same energy region with the same theoretical formulation [13].

The significant values of the nondipole parameter result from the fact that major dipole transitions, $4d \rightarrow \epsilon f$, have Cooper minima in this region, so the dipole amplitudes are anomalously small over a significant energy range, starting at about 100 eV in photoelectron energy. Because the dipole amplitudes appear in the denominator of the expressions for ζ, δ, and γ, these minima cause the nondipole parameters to be anomalously large. A similar effect is seen in Xe $5s$ photoionization [13, 24], but the energy range over which significant nondipole effects are exhibited is dramatically larger for Xe $4d$; ~ 100 eV for $4d$, as opposed to about 30 eV in the $5s$ case.

The large values and structure in ζ are signatures of interchannel coupling (configuration interaction in the continuum) with the $4p \rightarrow \epsilon f$ shape resonances in the quadrupole manifold [10]. This was demonstrated in Xe $5s$ and is quite evident in the theoretical curves shown in Fig. 2. The experimental structures are at higher energy, however, and the overall theoretical curves are qualitatively different; this indicates something of importance is omitted from theory.

Previous work has shown RRPA does an excellent job on the integrated cross section [25], the $\sigma_{4d_{5/2}}$: $\sigma_{4d_{3/2}}$ branching ratio [25] and the dipole photoelectron angular-distribution asymmetry parameter β, even to the extent of beautifully reproducing the experimental results for $4d_{3/2}$ and $4d_{5/2}$ individually over the same broad energy range considered here [23]. These agreements show conclusively that the $4d$ *dipole* photoionization channels are handled very well by RRPA. Thus, the

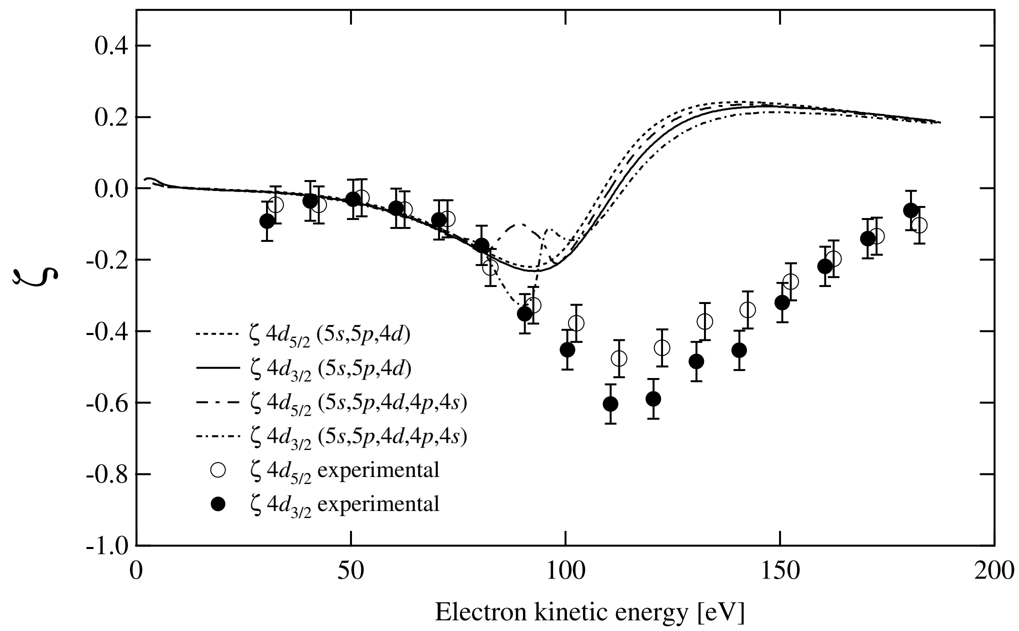

FIG. 2: Experimental and theoretical nondipole photoelectron angular-distribution parameter ζ for Xe $4d_{5/2}$ and $4d_{3/2}$ subshells.

difficulty must be in the *quadrupole* channels.

But, in the quadrupole manifold, *all* relevant single ionization channels are included, along with the interchannel coupling among them. Therefore, the only thing left, omission of multiple excitation channels within the quadrupole manifold, i.e., quadrupole satellite transitions, must be the principal reason for the experimental-theoretical discrepancy seen in Fig. 2.

It is known the $4p^5 4d^{10} 5s^2 5p^6\ {}^2P$ states of Xe$^+$ are *very* strongly mixed with $4p^6 4d^8 4f 5s^2 5p^6\ {}^2P$ states [26], i.e., $4p$ ionization is strongly mixed with ionization plus excitation from $4d$. Because, in the energy region of interest, the $4p \to \epsilon f$ shape resonances are the dominant transitions in the quadrupole manifold, interchannel coupling with these $4p$ ionization channels is crucial to a correct description of the $4d$ quadrupole ionization channels. In particular, the $4d$ satellites from transitions to the $4p^6 4d^8 4f 5s^2 5p^6 \epsilon f\ {}^1D$ states, which contain the resonant $4d \to \epsilon f$ ionizations, must be included for a correct description of $4d$ quadrupole ionization. In other words, analysis of the experimental and theoretical results leads us inescapably to the importance of interchannel coupling with satellite transitions within the quadrupole manifold.

But why should the $4d^8 4f \epsilon \ell$ channels be important for quadrupole photoionization but not nearly as important in the dipole manifold? Because, in the quadrupole manifold, the single excitation channels to the $4d^9 \epsilon \ell$ ($\ell = s, d, g$) states are nonresonant, while the excitation plus ionization channels to the $4d^8 4f \epsilon f$ states contain the resonant $4d \to \epsilon f$ transitions, giving the latter satellite channels extra clout within the quadrupole manifold. In the dipole manifold, just the reverse is true and the single excitation $4d^9 \epsilon f$ shape resonance dominates. Furthermore, using multiconfiguration Hartree-Fock (MCHF) theory [27], we have found the $4d^8 4f$ channels are spread out over a range of more than 10 eV non-relativistically, so with spin-orbit effects included, the spread should be close to about 20 eV. In addition, the quadrupole cross section of the satellite, which arises from the $4d \to \epsilon f$ shape resonance should be fairly broad. Thus, the spread of the $4d^8 4f$ thresholds, combined with the broadness of the ϵf resonant cross sections, means interchannel coupling with the main $4d^9$ quadrupole channels should be significant over a large energy range, thereby explaining why the structures observed in the $4d$ nondipole parameters are so wide.

It must also be explained why this same effect is not seen in Xe $5s$ photoionization [13, 24], where RRPA provides quite an accurate description of the nondipole effects. The answer lies in the strength of the interaction matrix element coupling the quadrupole satellite final continuum states, $4p^6 4d^8 4f 5s^2 5p^6 \epsilon f\ {}^1D$, with the main transition to $4p^6 4d^{10} 5s 5p^6 \epsilon p\ {}^1D$, in the case of $5s$ ionization, and $4p^6 4d^9 5s^2 5p^6 \epsilon f {}^1D$ for $4d$ ionization. Fundamentally, the interchannel-coupling matrix element of the satellite with the main $4d$ transition is

$$< 4d\epsilon' d | \frac{1}{r_{12}} | 4f \epsilon f >, \tag{2}$$

which is fairly large because both discrete wave functions have the *same* principal quantum number [28]. On the other hand, the interchannel-coupling matrix element between the satellites and the main $5s$ transition is

$$\langle 4d^2\epsilon' d|\frac{1}{r_{12}}|4f5s\epsilon f\rangle, \tag{3}$$

which vanishes in lowest order. Thus, the $5s$ transitions cannot couple directly to the satellites so the coupling must be of higher order, therefore small, so the Xe $5s$ quadrupole transitions are not significantly affected by the $4d$ satellites.

In conclusion then, the first measurement of individual nondipole parameters for a spin-orbit doublet has been performed, and dynamical effects of the spin-orbit interaction are seen. Significant nondipole effects are found at relatively low energy as a result of Cooper minima in dipole channels and interchannel coupling in quadrupole channels. Most importantly, sharp disagreement between experiment and theory, when otherwise excellent agreement was expected, has provided the first evidence of satellite two-electron quadrupole photoionizing transitions, along with their crucial importance for a quantitatively accurate theory. Our results point to the need of a theoretical method which simultaneously treats discrete-state correlation in initial and final-ionic states, interchannel coupling amongst the various ionization channels, relativistic interactions, both dipole and quadrupole transitions, and inner shells; all of which are required for a quantitative understanding of the Xe $4d$ nondipole parameters in this energy region.

The UNLV group acknowledges support by NSF Grant No. PHY-01-40375. DR acknowledges the financial support through the ALS Doctoral Fellowship in Residence program. The work of KTC was performed under the auspices of DOE by the University of California, LLNL under Contract No. W-7405-ENG-48. The research of WRJ was supported in part by NSF Grant No. PHY-01-39928. The research of HLZ was supported by NSF and NASA. The work of STM was supported by DOE, Division of Chemical Sciences, BES grant No. DE-FG02-03ER15428. The ALS (LBNL) was supported by DOE, Materials Science Division, BES, OER under Contract No. DE-AC03-76SF00098.

[1] D. W. Lindle and O. Hemmers, J. Electron Spectrosc. **100**, 297 (1999).
[2] A. Bechler and R. H. Pratt, Phys. Rev. A **39**, 1774 (1989); **42**, 6400 (1990).
[3] J. W. Cooper, Phys. Rev. A **42**, 6942 (1990); **45**, 3362 (1992); **47**, 1841 (1993).
[4] B. Krässig, M. Jung, D. S. Gemmell, E. P. Kanter, T. LeBrun, S. H. Southworth, and L. Young, Phys. Rev. Lett. **75**, 4736 (1995); M. Jung, B. Krässig, D. S. Gemmell, E. P. Kanter, T. LeBrun, S. H. Southworth, and L. Young, Phys. Rev. A **54**, 2127 (1996).
[5] O. Hemmers, G. Fisher, P. Glans, D. L. Hansen, H. Wang, S. B. Whitfield, R. Wehlitz, J. C. Levin, I. A. Sellin, R. C. C. Perera, E. W. B. Dias, H. S. Chakraborty, P. C. Deshmukh, S. T. Manson, and D. W. Lindle, J. Phys. B **30**, L727 (1997).
[6] N. L. S. Martin, D. B. Thompson, R. P. Bauman, C. D. Caldwell, M. O. Krause, S. P. Frigo, and M. Wilson, Phys. Rev. Lett. **81**, 1199 (1998).
[7] V. K. Dolmatov and S. T. Manson, Phys. Rev. Lett. **83**, 939 (1999).
[8] A. Derevianko, O. Hemmers, S. Oblad, P. Glans, H. Wang, S. B. Whitfield, R. Wehlitz, I. A. Sellin, W. R. Johnson, and D. W. Lindle, Phys. Rev. Lett. **84**, 2116 (2000).
[9] M. Ya. Amusia, A. S. Baltenkov, L. V. Chernysheva, Z. Felfli, and A. Z. Msezane, Phys. Rev. A **63**, 052506 (2001).
[10] W. R. Johnson and K. T. Cheng, Phys. Rev. A **63**, 022504 (2001).
[11] B. Krässig, E P Kanter, S. H. Southworth, R. Guillemin, O. Hemmers, D. W. Lindle, R. Wehlitz, and N. L. S. Martin, Phys. Rev. Lett. **88**, 203002 (2002).
[12] N. A Cherepkov and S. K. Semenov, J. Phys. B **34**, L495 (2001).
[13] O. Hemmers, R. Guillemin, E. P. Kanter, B. Krässig, D. W. Lindle, S. H. Southworth, R. Wehlitz, J. Baker, A. Hudson, M. Lotrakul, D. Rolles, W. C. Stolte, I. C. Tran, A. Wolska, S. W. Yu, M. Ya. Amusia, K. T. Cheng, L. V. Chernysheva, W. R. Johnson, and S. T. Manson, Phys. Rev. Lett. **91**, 053002 (2003).
[14] A. F. Starace, in *Handbuch der Physik*, v. 31, edited by W. Mehlhorn (Springer-Verlag, Berlin, 1982).
[15] M. Ya. Amusia, *Atomic Photoeffect* (Plenum Press, New York, 1990).
[16] M. Ya. Amusia, P. U. Arifov, A. S. Baltenkov, A. A. Grinberg, and S. G. Shapiro, Phys. Lett. **47A**, 66 (1974).
[17] M. Peshkin, Adv. Chem. Phys. **18**, 1 (1970).
[18] M. Ya. Amusia and V. K. Dolmatov, Sov. Phys. JETP **52**, 840 (1980).
[19] A. Derevianko and W. R. Johnson, At. Data Nuc. Data Tables **73**, 153 (1999).
[20] O. Hemmers, S. B. Whitfield, P. Glans, H. Wang, D. W. Lindle, R. Wehlitz, and I. A. Sellin, Rev. Sci. Instrum. **69**, 3809 (1998).
[21] W. R. Johnson and C. D. Lin, Phys. Rev. A **20**, 964 (1979).
[22] W. R. Johnson, C. D. Lin, K. T. Cheng, and C. M. Lee, Phys. Scr. **21**, 409 (1980).
[23] H. Wang, G. Snell, O. Hemmers, M. M. Sant'Anna, I. Sellin, N. Berrah, D. W. Lindle, P. C. Deshmukh, N. Haque, and S. T. Manson, Phys. Rev. Lett. **87**, 123004 (2001).
[24] S. Ricz, R. Sankari, Á. Kövér, M. Jurvansuu, D. Varga, J. Nikkinen, T. Ricsoka, H. Aksela, and S. Aksela, Phys. Rev. A **67** 012712 (2003).
[25] V. Schmidt, Rep. Prog. Phys. **55**, 1483 (1992) and references therein.
[26] H. Smid and J. Hansen, J. Phys. B **20**, 6541 (1987).
[27] C. Froese Fischer, Comput. Phys. Comm. **64**, 369 (1991).
[28] E. W. B. Dias, H. S. Chakraborty, P C Deshmukh, S. T. Manson, O. Hemmers, P. Glans, D. L. Hansen, H. Wang, S. B. Whitfield, D. W. Lindle, R. Wehlitz, J. C. Levin, I. A. Sellin, and R. C. C. Perera, Phys. Rev. Lett. **78**, 4553 (1997).